Chapter 2
Passivity As a Design Tool for Cooperative Control

2.1 Introduction

In this chapter, we formulate a coordination problem that is applicable to formation stabilization and group agreement as special cases, and present a class of feedback laws that solve this problem with local information. A key observation is that bidirectional communication gives rise to Structure 4 in Section 1.5, which guarantees that the resulting feedback loop will inherit the *passivity* properties of its components. By exploiting this structure, we develop a design method which results in a broad class of feedback laws that achieve passivity and, thus, stability of the interconnected system. The passivity approach also leads to a systematic construction of a Lyapunov function in the form of a sum of storage functions for the subsystems. As detailed in this chapter, several existing feedback rules for formation stability and group agreement become special cases in the passivity framework.

The coordination task studied in this chapter is to steer the differences between the output variables of group members to a prescribed compact set. This compact set may be a sphere when the outputs are positions of vehicles that must maintain a given distance in a formation, or the origin if the outputs are variables that must reach an agreement across the group. We thus formulate this task as a *set stability* problem and use passivity as a tool for constructing a stabilizing feedback law and a Lyapunov function with respect to this set. We prove global asymptotic stability with additional assumptions that guarantee appropriate *detectability* properties for trajectories away from the set.

2.2 Problem Statement

Consider a group of N agents, where each agent $i = 1, \cdots, N$, is represented by a vector $x_i \in \mathbb{R}^p$ that consists of variables to be coordinated with the rest of the group. The topology of information exchange between these agents is modeled as a graph

G. Since the information flow between neighbors is assumed to be bidirectional, G is an undirected graph. We also assume that G is connected and that G has ℓ undirected links. To simplify the analysis, we assign an orientation to G by considering one of the nodes to be the positive end of the link. As discussed in Section 1.4, the choice of orientation does not change the results because of the symmetric information flow.

The objective is to develop coordination laws that are implementable with local information (agent i can use the information of agent j if agent j is a neighbor) and that guarantee the following *two* group behaviors:

A1) Each agent achieves in the limit a common velocity vector $v(t) \in \mathbb{R}^p$ prescribed for the group; that is

$$\lim_{t \to \infty} |\dot{x}_i - v(t)| = 0, \quad i = 1, \cdots, N; \tag{2.1}$$

A2) If agents i and j are connected by link k, then the difference variable z_k

$$z_k := \sum_{l=1}^{N} d_{lk} x_l = \begin{cases} x_i - x_j \ \text{if } k \in \mathscr{L}_i^+ \\ x_j - x_i \ \text{if } k \in \mathscr{L}_i^- \end{cases} \tag{2.2}$$

converges to a prescribed compact set $\mathscr{A}_k \subset \mathbb{R}^p$, $k = 1, \cdots, \ell$, where d_{ik} is defined in (1.21).

The reference velocity $v(t)$ can be considered as a "mission plan" of the group. By specifying different $v(t)$, we achieve different group motions, such as rotational and translational motions. Examples of target sets $\mathscr{A}_k$ include the origin if x_i's are variables that must reach an agreement within the group, or a sphere in $\mathbb{R}^p$ if x_i's are positions of vehicles that must maintain a prescribed distance. Objectives A1-A2 may be employed to design and stabilize a formation of vehicles, or to synchronize variables in a distributed network of satellites, etc.

We introduce the concatenated vectors

$$x := [x_1^T, \cdots, x_N^T]^T \in \mathbb{R}^{pN} \quad z := [z_1^T, \cdots, z_\ell^T]^T \in \mathbb{R}^{p\ell}. \tag{2.3}$$

We partition D in terms of columns vectors, i.e.,

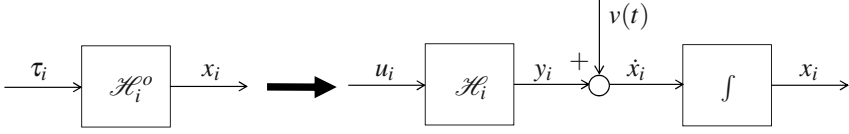$$D = [\, D_1 \,\vdots\, \cdots \,\vdots\, D_\ell \,] \tag{2.4}$$

and note from (2.2) that

$$z_k = (D_k^T \otimes I_p)x. \tag{2.5}$$

Concatenating z_k's together, we have

$$z = (D^T \otimes I_p)x \tag{2.6}$$

which means that z is restricted to be in the range space $\mathscr{R}(D^T \otimes I_p)$. Thus, for the objective A2 to be feasible, the target sets $\mathscr{A}_k$ must satisfy

$$\{\mathscr{A}_1 \times \cdots \times \mathscr{A}_\ell\} \cap \mathscr{R}(D^T \otimes I_p) \neq \emptyset. \tag{2.7}$$

Fig. 2.1 Step 1 transforms agent dynamics from (2.9) to (2.10) by designing an internal feedback τ_i. This internal feedback achieves for agent i passivity from an external feedback signal u_i to the velocity error y_i. The resulting passive block is denoted by $\mathscr{H}_i$.

2.3 The Passivity-based Design Procedure

Step 1. Design an internal feedback *loop for each agent $i = 1, \cdots, N$ that renders its dynamics passive from an external feedback signal u_i (to be designed in Step 2) to the velocity error*

$$y_i := \dot{x}_i - v(t). \tag{2.8}$$

Assume that the input-output dynamics of agent i are given by

$$x_i = \mathscr{H}_i^o\{\tau_i\}, \tag{2.9}$$

where $\mathscr{H}_i^o\{\tau_i\}$ denotes the output of a dynamic system $\mathscr{H}_i^o$ with the control input τ_i. The system $\mathscr{H}_i^o$ may be linear (e.g., single/double integrators) or nonlinear (e.g., Euler-Lagrange equation). In Step 1, we seek a feedback controller τ_i for each agent such that the agent dynamics $\mathscr{H}_i^o$ in (2.9) may be expressed as

$$\dot{x}_i = \mathscr{H}_i\{u_i\} + v(t), \tag{2.10}$$

where $\mathscr{H}_i$ is as in Fig. 2.1. For example, for the first order agent dynamics $\dot{x}_i = \tau_i$, Step 1 is trivially accomplished by choosing $\tau_i = \mathscr{H}_i\{u_i\} + v(t)$.

If $\mathscr{H}_i$ is dynamic, we assume that it is of the form

$$\mathscr{H}_i : \begin{cases} \dot{\xi}_i = f_i(\xi_i, u_i) \\ y_i = h_i(\xi_i, u_i) \end{cases} \tag{2.11}$$

where y_i is the velocity error and $\xi_i \in \mathbb{R}^{n_i}$ is the state variable of subsystem $\mathscr{H}_i$. We assume that $f_i(\cdot, \cdot)$ and $h_i(\cdot, \cdot)$ are C^2 functions such that

$$f_i(0, u_i) = 0 \Rightarrow u_i = 0 \tag{2.12}$$

and

$$h_i(0, 0) = 0. \tag{2.13}$$

The main restriction on (2.11) is that it be strictly passive with C^1, positive definite, radially unbounded storage functions $S_i(\xi_i)$ satisfying (1.27) for some positive definite functions $W_i(\cdot)$.

If $\mathscr{H}_i$ is a static block, we restrict it to be of the form

$$y_i = h_i(u_i) \tag{2.14}$$

where $h_i : \mathbb{R}^p \to \mathbb{R}^p$ is a locally Lipschitz function satisfying (1.25) for any $u \neq 0$. In the situation where one of the agents, say agent 1, is the "leader" of the group in the sense that $\dot{x}_1$ uses no feedback term from the other agents, we let

$$h_1(u_1) \equiv 0 \quad \forall u_1 \in \mathbb{R}^p. \tag{2.15}$$

We next show how to apply Step 1 to agents modeled as double integrators. In Chapters 5 and 6, we will demonstrate that broader classes of physical systems, including rigid body rotation and Euler-Lagrange systems in (1.34), may be transformed to the form in Step 1.

Example 2.1 (Step 1 for agents modeled as double integrators).
   We consider double integrator agent dynamics

$$m_i \ddot{x}_i = \tau_i, \quad i = 1, \cdots, N \tag{2.16}$$

where m_i is the mass of agent i, $x_i \in \mathbb{R}^p$ denotes the position of agent i and $\tau_i \in \mathbb{R}^p$ is the force input of agent i. For planar agents, $p = 2$ and for spatial agents, $p = 3$.
   According to Step 1, we design an internal feedback

$$\tau_i = -k_i(\dot{x}_i - v(t)) + m_i \dot{v}(t) + u_i, \quad k_i > 0 \tag{2.17}$$

which makes use of information available only to agent i itself. This feedback law, together with the change of variables

$$\xi_i = \dot{x}_i - v(t), \tag{2.18}$$

brings (2.16) to the form

$$\dot{x}_i = y_i + v(t) \tag{2.19}$$

$$\mathscr{H}_i : \begin{cases} m_i \dot{\xi}_i = -k_i \xi_i + u_i \\ y_i = \xi_i. \end{cases} \tag{2.20}$$

Note that $\mathscr{H}_i$ is first order because we effectively consider ξ_i as the state variable instead of x_i. The transfer matrix of (2.20) from u_i to y_i is

$$H_i(s) = \frac{1}{m_i s + k_i} I_p, \quad k_i > 0, \tag{2.21}$$

which is strictly positive real as shown in Example 1.4. Thus, $\mathscr{H}_i$ is strictly passive due to Lemma 1.2. Indeed, a valid storage function for (2.20) is given by

$$S_i(\xi_i) = \frac{1}{2} m_i \xi_i^T \xi_i. \tag{2.22}$$

It is easy to examine that the assumptions in (2.12) and (2.13) are satisfied in (2.20). Thus, Step 1 is completed with the control law in (2.17). Note that other higher order control laws can be designed to render $\mathscr{H}_i$ strictly passive. □

Step 2. Design an external feedback *signal u_i of the form*

$$u_i = -\sum_{k=1}^{\ell} d_{ik} \psi_k(z_k) \tag{2.23}$$

where z_k's are the relative variables as in (2.2), and the multivariable nonlinearities $\psi_k : \mathbb{R}^p \to \mathbb{R}^p$ are to be designed such that the target sets $\mathscr{A}_k$ are invariant and asymptotically stable.

The external feedback law (2.23) is decentralized and implementable with available information since $d_{ik} \neq 0$ only when link k is connected to node i.

Before specifying the properties of ψ_k, we note from Fig. 2.1 and (2.23) that the interconnection of $\mathscr{H}_i$'s and ψ_k's is as in Fig. 2.2, where

$$u = [u_1^T, \cdots, u_N^T]^T \in \mathbb{R}^{pN} \quad \psi = [\psi_1^T, \cdots, \psi_\ell^T]^T \in \mathbb{R}^{p\ell} \quad y = [y_1^T, \cdots, y_N^T]^T \in \mathbb{R}^{pN}. \tag{2.24}$$

Note from (2.23) that

$$u_i = -[\, d_{i1}I_p \mid \cdots \mid d_{i\ell}I_p \,]\psi, \tag{2.25}$$

which means

$$u = -(D \otimes I_p)\psi(z). \tag{2.26}$$

Fig. 2.2 exhibits a "symmetric" interconnection structure similar to Structure 4 in Section 1.5. The symmetric interconnection follows from the symmetry inherent in the undirected graphs. This structure allows us to proceed with a passivity-based design of ψ_k, $k = 1, \cdots, \ell$.

We design the nonlinearities $\psi_k(z_k)$ to be of the form

$$\psi_k(z_k) = \nabla P_k(z_k) \tag{2.27}$$

where $P_k(z_k)$ is a nonnegative C^2 function

$$P_k : \mathscr{G}_k \to \mathbb{R}_{\geq 0} \tag{2.28}$$

defined on an open set $\mathscr{G}_k \subseteq \mathbb{R}^p$, where z_k is allowed to evolve. As an illustration, if x_i's are positions of point masses that must maintain a prescribed distance, then the choice $\mathscr{G}_k = \{z_k \mid z_k \in \mathbb{R}^p \setminus 0\}$ disallows the possibility of collisions between linked agents.

To steer z_k's into the target sets $\mathscr{A}_k \subset \mathscr{G}_k$, we let $P_k(z_k)$ and its gradient $\nabla P_k(z_k)$ vanish on $\mathscr{A}_k$, and let $P_k(z_k)$ grow unbounded as z_k goes to the boundary of $\mathscr{G}_k$:

$$P_k(z_k) \to \infty \text{ as } z_k \to \partial \mathscr{G}_k \tag{2.29}$$

$$P_k(z_k) = 0 \Leftrightarrow z_k \in \mathscr{A}_k \tag{2.30}$$

$$\nabla P_k(z_k) = 0 \Leftrightarrow z_k \in \mathscr{A}_k. \tag{2.31}$$
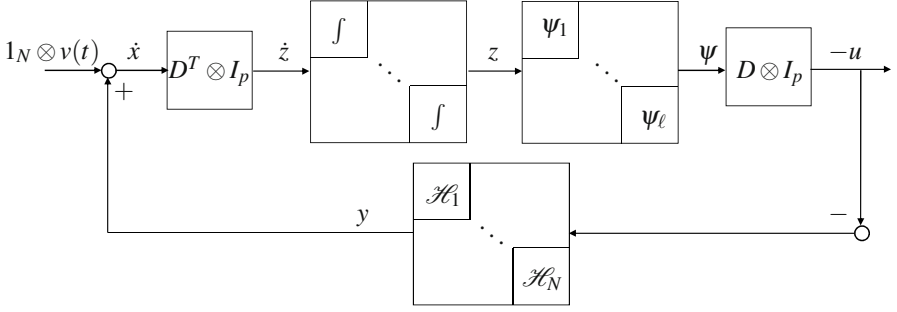
Fig. 2.2 The closed-loop structure of (2.8), (2.11) and (2.26): $\mathscr{H}_i$'s are designed to be strictly passive while pre- and post-multiplying D^T and D preserves the passivity from $\dot{z}$ to ψ. The closed-loop stability follows from the interconnection of two passive systems.

When $\mathscr{G}_k = \mathbb{R}^p$, (2.29) means that $P_k(z_k)$ is radially unbounded. As shown in [137, Remark 2], a continuous function $P_k(z_k)$ satisfying (2.29) and (2.30) exists for any given open set $\mathscr{G}_k$ and compact subset $\mathscr{A}_k \subset \mathscr{G}_k$. We further assume that the sets $\mathscr{A}_k$ and $\mathscr{G}_k$ are chosen such that C^2 smoothness of $P_k(\cdot)$ and (2.31) are also achievable.

For example, if two agents need to reach a common value, we let $\mathscr{A}_k = \{0\}$ and $\mathscr{G}_k = \mathbb{R}^p$. Then the choice of $P_k(z_k) = \frac{1}{2}|z_k|^2$ satisfies (2.28)-(2.31). If two agents must maintain a relative distance of 1, we may choose $\mathscr{A}_k = \{z_k \mid |z_k| = 1\}$ and $\mathscr{G}_k = \{z_k \mid z_k \in \mathbb{R}^p \setminus 0\}$. In this case, a valid choice of P_k is given by $P_k(z_k) = |z_k| - \ln|z_k| - 1$.

The construction of ψ_k as in (2.27) is designed to render the system from $\dot{z}_k$ to ψ_k (and hence from $\dot{z}$ to ψ due to the block diagonal structure in Fig. 2.2) passive. Indeed, consider P_k as a storage function and note that

$$\dot{P}_k = \psi_k(z_k)^T \dot{z}_k, \tag{2.32}$$

which shows the passivity property.

2.4 Stability Results

From Fig. 2.2, the set of equilibria is given by

$$\mathscr{E} = \left\{ (z, \xi) \mid \xi = 0, \ (D \otimes I_p)\psi(z) = 0 \text{ and } z \in \mathscr{R}(D^T \otimes I_p) \right\} \tag{2.33}$$

which means that the following property must hold true to ensure that no equilibria arises outside the sets $\mathscr{A}_k$:

Property 2.1. For any $(z,0) \in \mathscr{E}$, i.e., $\xi = 0$, $(D \otimes I_p)\psi(z) = 0$ and $z \in \mathscr{R}(D^T \otimes I_p)$, z satisfies $z \in \mathscr{A}_1 \times \cdots \times \mathscr{A}_\ell$. $\square$

In view of (2.26), Property 2.1 means that

$$u = 0 \Longleftrightarrow z = (D^T \otimes I_p)x \in \mathscr{A}_1 \times \ldots \times \mathscr{A}_\ell. \tag{2.34}$$

When the graph has no cycles, that is, when the columns of D are linearly independent, then $(D \otimes I_p)\psi(z) = 0$ implies $\psi(z) = 0$ and $z_k \in \mathscr{A}_k$ follows from (2.31). Thus, Property 2.1 holds for acyclic graphs. When the columns of D are linearly dependent, whether Property 2.1 holds depends on the sets $\mathscr{A}_k$ and ψ_k. As we will illustrate, it holds in agreement problems where $\mathscr{A}_k$ is the origin but fails in the formation control problem with distance only criterion where $\mathscr{A}_k$ is a sphere.

The feedback interconnection shown in Fig. 2.2 is of the same form as Structure 4 in Section 1.5. The storage functions for the feedforward and feedback subsystems of Fig. 2.2 are, respectively,

$$V_f(z) := \sum_{i=1}^{\ell} P_k(z_k) \quad \text{and} \quad V_b(\xi) := \sum_{i \in \mathscr{I}} S_i(\xi_i) \tag{2.35}$$

where $\mathscr{I}$ denotes the subset of indices $i = 1, \cdots, N$ that correspond to dynamic blocks $\mathscr{H}_i$. In particular, the passivity of the feedforward subsystems follows from Structure 1 in Section 1.5. Using the passivity of the feedforward and feedback subsystems and Structure 4 in Section 1.5 and imposing Property 2.1, we prove asymptotic stability of the set of points where $\xi = 0$ and $z_k \in \mathscr{A}_k$ by taking as a Lyapunov function the sum of the two storage functions in (2.35). This construction results in a Lur'e-type Lyapunov function because its key ingredient $P_k(z_k)$ is the integral of the feedback nonlinearity $\psi_k(z_k) = \nabla P_k(z_k)$. We summarize the main stability result in the following theorem.

Theorem 2.1. *Consider the closed-loop system (2.8), (2.11) and (2.23), where $v(t)$ is uniformly bounded and piecewise continuous and $\mathscr{H}_i$, $i = 1, \cdots, N$, and ψ_k, $k = 1, \cdots, \ell$ are designed as in (2.11)-(2.15) and (2.27)-(2.31) for given open sets $\mathscr{G}_k \subseteq \mathbb{R}^p$ and compact subsets $\mathscr{A}_k \subset \mathscr{G}_k$, where $\mathscr{A}_k$ are as in (2.7). Then:*
i) The feedforward path in Fig. 2.2 is passive from $\dot{x}$ to $-u$, and from y to u;
ii) The feedback path is passive from input u to y;
iii) When Property 2.1 holds, the set

$$\mathscr{A} = \left\{ (z, \xi) \mid \xi = 0, z \in \mathscr{A}_1 \times \cdots \times \mathscr{A}_\ell \cap \mathscr{R}(D^T \otimes I_p) \right\} \tag{2.36}$$

is uniformly asymptotically stable with region of attraction

$$\mathscr{G} = \left\{ (z, \xi) \mid \xi \in \mathbb{R}^{n_1} \times \cdots \times \mathbb{R}^{n_N}, z \in \mathscr{G}_1 \times \cdots \times \mathscr{G}_\ell \cap \mathscr{R}(D^T \otimes I_p) \right\}. \tag{2.37}$$

Moreover, all trajectories $(z(t), \xi(t))$ starting in $\mathscr{G}$ converge to the set of equilibria $\mathscr{E}$ in (2.33). □

When Property 2.1 fails, Theorem 2.1 proves that all trajectories converge to the set of equilibria $\mathscr{E}$ in (2.33). In this case, it is possible to conclude "generic convergence" to $\mathscr{A}$ from almost all initial conditions if one can show that the equilibria outside of $\mathscr{A}$ are unstable. We will illustrate such an example in Section 2.7.

Convergence to $\mathscr{A}$ means that the difference variables z_k tend to the target sets $\mathscr{A}_k$. It also implies that $\xi = 0$, $u = 0$ and thus, y in (2.8) is zero, which means that both objectives A1 and A2 are indeed achieved.

Proof (Proof of Theorem 2.1).
   i) To prove passivity from $\dot{x}$ to $-u$ we use $V_f(z)$ in (2.35) as a storage function, and obtain from (2.27), (2.6), (2.26) and $(D \otimes I_p)^T = D^T \otimes I_p$:

$$\dot{V}_f = \psi^T \dot{z} = \psi^T (D^T \otimes I_p) \dot{x} = \{(D \otimes I_p)\psi\}^T \dot{x} = -u^T \dot{x}. \tag{2.38}$$

To show passivity from y to $-u$ we substitute $\dot{x} = 1_N \otimes v(t) + y$ in (2.38) and use the fact $(D^T \otimes I_p)(1_N \otimes v(t)) = 0$ from the third item in Property 1.5, thus obtaining

$$\dot{V}_f = \psi^T (D^T \otimes I_p)\{1_N \otimes v(t) + y\} = \psi^T (D^T \otimes I_p)y$$
$$= \{(D \otimes I_p)\psi\}^T y = -u^T y. \tag{2.39}$$

ii) To establish passivity of the feedback path, we let $\mathscr{I}$ denote the subset of indices $i = 1, \cdots, N$ for which $\mathscr{H}_i$ is a dynamic block as in (2.11), and employ the storage function $V_b(\xi)$ in (2.35), which yields:

$$\dot{V}_b = \sum_{i \in \mathscr{I}} \dot{S}_i \leq \sum_{i \in \mathscr{I}} (-W_i(\xi_i) + u_i^T y_i). \tag{2.40}$$

Adding to the right-hand side of (2.40)

$$\sum_{i \notin \mathscr{I}} u_i^T y_i \geq 0 \tag{2.41}$$

which is nonnegative because the static blocks satisfy (1.25) or (2.15), we get

$$\dot{V}_b \leq \sum_{i \in \mathscr{I}} (-W_i(\xi_i) + u_i^T y_i) + \sum_{i \notin \mathscr{I}} u_i^T y_i \leq -\sum_{i \in \mathscr{I}} W_i(\xi_i) + u^T y \tag{2.42}$$

and, thus, conclude passivity with input u and output y.
iii) To prove asymptotic stability of the set $\mathscr{A}$ we use the Lyapunov function

$$V(z, \xi) = V_f(z) + V_b(\xi) \tag{2.43}$$

which is zero on the set $\mathscr{A}$ due to property (2.30), and grows unbounded as (z, ξ) approaches $\partial \mathscr{G}^\infty$ due to property (2.29). From (2.39), (2.40) and (2.41), this Lyapunov function yields the negative semidefinite derivative

$$\dot{V} \leq -\sum_{i \in \mathscr{I}} W_i(\xi_i) - \sum_{i \notin \mathscr{I}} u_i^T y_i, \tag{2.44}$$

which implies that the trajectories $(z(t), \xi(t))$ are bounded on $t \in [0, T]$, for any T within the maximal interval of definition $[0, t_f)$ for the differential equations (2.8), (2.11). Because this bound does not depend on T, and because $v(t)$ is bounded, from

(2.8) we can find a bound on $x(t)$ that grows linearly in T. This proves that there is no finite escape time because, if t_f were finite, by letting $T \to t_f$ we would conclude that $x(t_f)$ exists, which is a contradiction.

Having proven the existence of solutions for all $t \geq 0$, we conclude from (2.44) stability of the set $\mathscr{A}$. However, because the right-hand side of (2.44) vanishes on a superset of $\mathscr{A}$, to prove attractivity of $\mathscr{A}$ we appeal to the Invariance Principle[1] reviewed in Appendix B.2. To investigate the largest invariant set where $\dot{V}(z, \xi) = 0$ we note from (2.12) that if $\xi_i = 0$ holds identically then $u_i = 0$. Likewise the static blocks satisfy (1.25) or (2.15), which means that the right-hand side of (2.44) vanishes when $u_i = 0$, $i = 1, \cdots, N$. Indeed, if the first member $i = 1$ satisfies (1.25), then $u_1 = 0$ follows directly. If it satisfies (2.15) instead of (1.25), $u_1 = 0$ still holds because the sum of the rows of D being zero implies, from (2.6), that

$$u_1 = -\sum_{i=2}^{N} u_i = 0. \tag{2.45}$$

We thus conclude that $u = 0$, which means from (2.26) that $\psi(z)$ lies in the null space $\mathscr{N}(D \otimes I_p)$. Using the Invariance Principle, which states that all bounded solutions approach their positive limit set, which is invariant, we conclude that the trajectories converge to the set $\mathscr{E}$ in (2.33). When Property 2.1 holds, $\mathscr{E}$ coincides with $\mathscr{A}$, which proves asymptotic stability of $\mathscr{A}$ with region of attraction $\mathscr{G}$, while uniformity of asymptotic stability follows from the time-invariance of the (z, ξ)-dynamics. $\square$

The Lyapunov function $V(z, \xi)$ in the proof above yields a negative semidefinite derivative. By using the observability condition in (2.12), we prove the stability results in Theorem 2.1. This Lyapunov function allows us to develop different adaptive schemes to enhance robustness of group motion. For example, in Chapters 3 and 4, we develop adaptive schemes that enable agents to estimate leader's mission plan $v(t)$. These adaptive schemes relax the assumption in Theorem 2.1 that all the agents must have the $v(t)$ information. In Chapter 6, where agreement of multiple Euler-Lagrange systems is studied, we attempt to design adaptive control laws from $V(z, \xi)$ to compensate for uncertainties in Euler-Lagrange systems. However, we illustrate with an example that the resulting adaptive design is not sufficient to ensure group objectives. This is because $\dot{V}$ is only negative *semidefinite*. We will detail in Chapter 6 how we overcome this insufficiency by exploiting the structure of Euler-Lagrange equations and the design flexibility offered by the passivity-based framework.

---

[1] The Invariance Principle is indeed applicable because the dynamics of (z, ξ) are autonomous: Although $v(t)$ appears in the block diagram in Fig. 2.2, it is canceled in the $\dot{z}$ equation because $(D^T \otimes I_p)(1_N \otimes v(t)) = 0$.

2.5 Application to the Agreement Problem

In several cooperative tasks, it is of interest to steer group variables, such as position, heading, phase of oscillators, to a common value. To apply Theorem 2.1 to this problem, we let $x_i \in \mathbb{R}^p$ denote a vector of variables of interest, and select the target sets to be $\mathscr{A}_k = \{0\}$. With this choice of $\mathscr{A}_k$, the target set constraint (2.7) is trivially satisfied. We may choose $P_k(z_k)$ as a positive definite, radially unbounded function on $\mathscr{G}_k = \mathbb{R}^p$ with the property

$$z_k^T \nabla P_k(z_k) = z_k^T \psi_k(z_k) > 0 \quad \forall z_k \neq 0 \tag{2.46}$$

so that (2.27)-(2.31) and Property 2.1 hold. In particular, Property 2.1 holds because $z \in \mathscr{R}(D^T \otimes I_p)$ and $\psi(z) \in \mathscr{N}(D \otimes I_p)$ imply that z and $\psi(z)$ are orthogonal to each other, which, in view of (2.46), is possible only if $z = 0$.

Corollary 2.1. *Consider agents $i = 1, \cdots, N$, interconnected as described by the graph representation (1.21), and let z_k, $k = 1, \cdots, \ell$ denote the differences between the variables x_i of neighboring members as in (2.2). Let $P_k(z_k)$ be positive definite, radially unbounded functions satisfying (2.46) and let $\psi_k(z_k) = \nabla P_k(z_k)$. Then the agreement protocol*

$$\dot{x}_i = \mathscr{H}_i \left\{ -\sum_{i=1}^{\ell} d_{ik} \psi_k(z_k) \right\} + v(t), \quad i = 1, \cdots, N \tag{2.47}$$

where $\mathscr{H}_i\{u_i\}$ denotes the output at time t of a static or dynamic block satisfying (2.11)-(2.15), guarantees $|\dot{x}_i - v(t)| \to 0$ and

$$x_i - x_j \to 0 \quad as \quad t \to \infty \tag{2.48}$$

for every pair of nodes (i, j) which are connected by a path. □

When $p = 1$, that is when x_i's and z_k's are scalars, condition (2.46) means that $\psi_k(z_k) = \nabla P_k(z_k)$ is a *sector* nonlinearity which lies in the first and third quadrants. Corollary 2.1 thus encompasses the result of [102], which proposed agreement protocols of the form

$$\dot{x}_i = - \sum_{j \in \mathscr{N}_i} \phi_{ij}(x_i - x_j) \tag{2.49}$$

where $\phi_{ij}(\cdot) = \phi_{ji}(\cdot)$ plays the role of our $\psi_k(\cdot)$. However, both [102] and a related result in [122] assume that the nonlinearities $\phi_{ij}(\cdot)$ satisfy an *incremental sector* assumption which is more restrictive than the sector condition (2.46) of Corollary 2.1. An independent study in [147] takes a similar approach to synchronization as [122]; however, it further restricts the coupling terms $\phi_{ij}(\cdot)$ to be linear. The feedback law (2.47) in Corollary 2.1 generalizes (2.49) by applying to its right-hand side the additional operation $\mathscr{H}_i\{\cdot\}$, which may either represent a passive filter or another sector nonlinearity $h_i(\cdot)$ as specified in Section 2.3. Because $\mathscr{H}_i$ in (2.47) can be dynamic, Corollary 2.1 is applicable, unlike other agreement results surveyed

in [110], to plants with higher-order dynamics than an integrator. See, for example, the second order system in Section 2.6.1.

2.6 Position-based Formation Control As a Shifted Agreement Problem

One of the major topics in cooperative control is the formation maintenance and stability, where the goal is to drive relative positions (i.e., z_k's) or relative distances (i.e., $|z_k|$'s) between agents to prescribed values. Depending on the goal, we may pursue one of the following:

- *distance-based formation control*, where the desired target set $\mathscr{A}_k$ in objective A2 is given by
$$\mathscr{A}_k = \{z_k \mid |z_k| = d_k\}, \quad d_k \in \mathbb{R}_{>0}, \; k = 1, \cdots, \ell; \tag{2.50}$$

- *position-based formation control*, where the desired target set $\mathscr{A}_k$ in objective A2 is given by
$$\mathscr{A}_k = \{z_k \mid z_k = z_k^d\}, \quad z_k^d \in \mathbb{R}^p, \; k = 1, \cdots, \ell. \tag{2.51}$$

The goal of the distance-based formation control is to achieve a desired shape of the group formation while the position-based formation control concerns not only the desired shape but also the desired orientation of the group formation. We first consider the position-based formation control and demonstrate that it can be transformed to an agreement problem.

The set points z_k^d in (2.51) dictate the relative configuration of the group. When the graph contains cycles, the sum of the relative position vectors z_j over each cycle must be zero; that is, $z = [z_1^T, \cdots, z_\ell^T]^T$ must lie in the range space of $D^T \otimes I_p$ so that (2.7) holds. We thus assume that $z^d = [(z_1^d)^T, \cdots, (z_\ell^d)^T]^T$ is designed to lie in the range space of $D^T \otimes I_p$, which means that

$$z^d = (D^T \otimes I_p)x_c \tag{2.52}$$

for some $x_c \in \mathbb{R}^{pN}$. The condition (2.52) implies that (2.7) is satisfied.

Introducing

$$\mathbf{x}(t) := x(t) - x_c - \int_0^t \mathbf{1}_N \otimes v(\tau)d\tau, \tag{2.53}$$

where x_c is as in (2.52), and

$$\mathbf{z} = (D^T \otimes I_p)\mathbf{x} = z - z^d, \tag{2.54}$$

we notice that objectives A1-A2 for the position-based formation control translate to the asymptotic stability of the origin for

$$X = [\dot{\mathbf{x}}^T \; \mathbf{z}^T]^T. \tag{2.55}$$

According to Corollary 2.1, the global asymptotic stability of $X = 0$ is guaranteed by the protocol

$$\dot{\mathbf{x}}_i = \mathcal{H}_i \left\{ -\sum_{i=1}^{\ell} d_{ik} \psi_k(\mathbf{z}_k) \right\}, \quad i = 1, \cdots, N \tag{2.56}$$

where $\psi_k(\cdot)$ satisfies (2.46). Using (2.23), (2.53) and (2.54), we rewrite (2.56) in the original coordinate $(\dot{x}, z)$ as

$$\dot{x}_i = y_i + v(t) \tag{2.57}$$
$$y_i = \mathcal{H}_i\{u_i\} \tag{2.58}$$

where

$$u_i = -\sum_{i=1}^{\ell} d_{ik} \psi_k(z_k - z_k^d). \tag{2.59}$$

Corollary 2.2. *Consider a group of agents $i = 1, \cdots, N$. The protocol (2.57)-(2.58), where $\psi_k = \nabla P_k(z_k)$ satisfies (2.46), guarantees that*

$$|\dot{x}_i - v(t)| \to 0, \quad \forall i, \tag{2.60}$$

and

$$z_k \to z_k^d, \quad \forall k. \tag{2.61}$$

$\square$

Example 2.2 (Collision avoidance).
   The closed-loop system (2.57)-(2.58) ensures only the convergence to the desired formation. Other objectives, such as collision avoidance, can be achieved by incorporating additional feedback terms. For example, to avoid collision, we employ the artificial potential field approach in robotics and augment u_i in (2.58) as

$$u_i = -\sum_{k=1}^{\ell} d_{ik} \psi_k(z_k - z_k^d) - \sum_{j=1}^{N} \nabla_{x_i} Q_{ij}(|x_i - x_j|) \tag{2.62}$$

where the C^1 artificial potential function $Q_{ij}(\cdot) : \mathbb{R}_{\geq 0} \to \mathbb{R}_{\geq 0}$ satisfies

$$Q_{ij}(s) \to \infty \quad \text{as} \quad s \to 0 \tag{2.63}$$
$$Q_{ij}(s) = 0 \quad \text{as} \quad s > R \tag{2.64}$$

for some positive R. Using the Lyapunov function

$$V = \sum_{i=1}^{N} S_i(\xi_i) + \sum_{k=1}^{\ell} P_k(z_k - z_k^d) + \sum_{i=1}^{N} \sum_{j>i} Q_{ij}(|x_i - x_j|) \tag{2.65}$$

we obtain

$$\dot{V} \leq -\sum_{i=1}^{N} W_i(\xi) - \sum_{i=1}^{N} \left(y_i^T \sum_{j=1, j\neq i}^{N} \nabla_{x_i} Q_{ij}(|x_i - x_j|) \right)$$
$$+ \sum_{i=1}^{N} \sum_{j>i} \left((\nabla_{x_i} Q_{ij}(|x_i - x_j|))^T \dot{x}_i + (\nabla_{x_j} Q_{ij}(|x_i - x_j|))^T \dot{x}_j \right). \tag{2.66}$$

Since $\nabla_{x_i} Q_{ij}(|x_i - x_j|) = -\nabla_{x_j} Q_{ij}(|x_i - x_j|)$, we rewrite $\dot{V}$ using (2.57) as

$$\dot{V} \leq -\sum_{i=1}^{N} W_i(\xi) - \sum_{i=1}^{N} \sum_{j=1, j\neq i}^{N} y_i^T (\nabla_{x_i} Q_{ij}(|x_i - x_j|))$$
$$+ \sum_{i=1}^{N} \sum_{j>i} \left((\nabla_{x_i} Q_{ij}(|x_i - x_j|))^T y_i + (\nabla_{x_j} Q_{ij}(|x_i - x_j|))^T y_j \right)$$
$$= -\sum_{i=1}^{N} W_i(\xi) - \sum_{i=1}^{N} \sum_{j<i} y_i^T (\nabla_{x_i} Q_{ij}(|x_i - x_j|)) + \sum_{i=1}^{N} \sum_{j>i} (\nabla_{x_j} Q_{ij}(|x_i - x_j|))^T y_j$$
$$= -\sum_{i=1}^{N} W_i(\xi) \leq 0. \tag{2.67}$$

Thus, V in (2.65) is nonincreasing, that is, $V(t) \leq V(0)$. Since $V \to \infty$ as $|x_i - x_j| \to 0$, $\forall i \neq j$, the boundedness of $V(t)$ implies collision avoidance.

Applying the Invariance Principle, we conclude from (2.67) that $\xi \to 0$, which implies from (2.12) that $u \to 0$. Note that due to the additional term in (2.62) that handles collision avoidance, $u_i \to 0$ does not mean $z_k \to z_k^d$, that is, convergence to the desired formation is not guaranteed. Indeed, there may exist an asymptotically stable equilibrium where $u_i = 0$ and the desired formation is not achieved. This equilibrium corresponds to a local minimum of the potential function V in (2.65). To eliminate such a local minima, one may apply navigation function techniques in [113] to the construction of P_k and Q_{ij} such that from almost all initial conditions, the agents converge to the desired formation. We refer interested readers to [133, 132] for further details on applying navigation function to formation control. □

2.6.1 Design Example

We consider a group of agents modeled as (2.16) in Example 2.1. The feedback law (2.17) achieves Step 1. We next apply Step 2 and design u_i. According to Corollary 2.2, we take

$$u_i = -\sum_{i=1}^{\ell} d_{ik} \psi_k(z_k - z_k^d), \tag{2.68}$$

where $\psi_k(\cdot)$ satisfies (2.46). The closed-loop system of (2.19), (2.20) and (2.59) is given by

$$m_i(\ddot{x}_i - \dot{v}(t)) + k_i(\dot{x}_i - v(t)) + \sum_{i=1}^{\ell} d_{ik}\psi_k(z_k - z_k^d) = 0 \tag{2.69}$$

which can be rewritten as

$$(M \otimes I_p)\ddot{\mathbf{x}} + (K \otimes I_p)\dot{\mathbf{x}} + (D \otimes I_p)\psi(\mathbf{z}) = 0 \tag{2.70}$$

where $M = \mathrm{diag}\{m_1, \cdots, m_N\}$ and $K = \mathrm{diag}\{k_1, \cdots, k_N\}$.

We now show that for quadratic potential function P_k, (2.70) recovers a second order linear consensus protocol. To this end, we choose a quadratic potential function

$$P_k = \frac{\delta_k}{2}|z_k - z_k^d|^2 \quad \delta_k \in \mathbb{R}_{>0} \tag{2.71}$$

which leads to

$$\psi_k(z_k) = \delta_k(z_k - z_k^d). \tag{2.72}$$

The constants δ_k's are the feedback gains which regulate the relative emphasis of $|z_k - z_k^d|$ for different k's. Defining

$$\Delta = \mathrm{diag}\{\delta_1, \cdots, \delta_\ell\} \tag{2.73}$$

and substituting (2.54) in (2.70), we obtain

$$(M \otimes I_p)\ddot{\mathbf{x}} + (K \otimes I_p)\dot{\mathbf{x}} + (L_\Delta \otimes I_p)\mathbf{x} = 0 \tag{2.74}$$

where $L_\Delta = D\Delta D^T$ is the *weighted* graph Laplacian (recall that without the subscript "Δ", L denotes the *unweighted* Laplacian $L = DD^T$). The closed-loop system (2.74) is a second order linear consensus protocol well studied in the literature (see e.g., [109]). The design in (2.70) gives a passivity interpretation of the second order consensus protocol (2.74) and extends it to nonlinear coupling ψ_k.

Example 2.3 (Agreement of Second-order Agents with Directed Graphs).

When the graph is undirected, the stability of (2.74) holds for arbitrary $m_i > 0$ and $k_i > 0$, $\forall i$. For directed graphs, however, (2.74) may become unstable even for uniform m_i and k_i. To illustrate this, let us take $p = 1$ (scalar variables), $m_i = 1$, $k_i = 1$, and $\delta_k = 1$, $\forall i$, $\forall k$, in (2.74), which leads to

$$\ddot{\mathbf{x}} + \dot{\mathbf{x}} + L\mathbf{x} = 0 \tag{2.75}$$

where L is defined in (1.11).

To investigate the stability of (2.75), we use the Schur decomposition reviewed in Appendix B.1 and decompose L as

$$L = QBQ^{-1} \tag{2.76}$$

where Q is a unitary complex matrix and B is an upper triangular matrix with all the eigenvalues of L on the diagonal of B. Note that if L is symmetric, i.e., the graph G is undirected, Q can chosen as the orthonormal eigenvectors of L and accordingly B
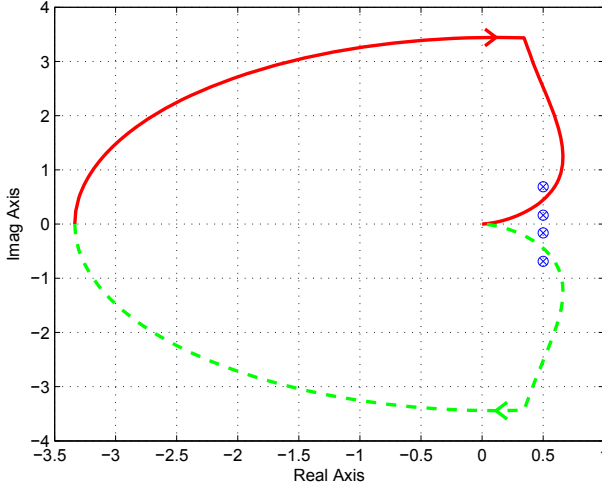
Fig. 2.3 Nyquist plot of $-\frac{1}{s(s+1)}$. Four $\otimes$'s denote the inverse of four nonzero eigenvalues of the graph Laplacian matrix when the information topology is a directed cycle of 5 agents.

is a diagonal matrix. We will use this decomposition technique again in Chapter 9 to study robustness properties of (2.74) with undirected graphs.

Using a coordinate transformation

$$d = Q^{-1}\mathbf{x}, \tag{2.77}$$

we obtain from (2.75)

$$\ddot{d} + \dot{d} + Bd = 0, \quad i = 1, \cdots, N. \tag{2.78}$$

Because B is upper triangular and because the eigenvalues of L are the diagonal elements of B, the stability of (2.78) is equivalent to the stability of

$$\ddot{d} + \dot{d} + \lambda_i d = 0, \quad i = 1, \cdots, N, \tag{2.79}$$

where λ_i is the ith eigenvalue of L. If $\lambda_i = 0$ for some i, (2.79) is stable. It then follows that (2.79) (and thus (2.75)) is stable if and only if the Nyquist plot of $-\frac{1}{s(s+1)}$ does not encircle λ_i^{-1} for any nonzero λ_i.

The Nyquist plot of $-\frac{1}{s(s+1)}$ is shown by the solid-dash line in Fig. 2.3. For undirected graphs, λ_i is nonnegative and the Nyquist plot never encircles nonnegative real axis. Therefore, the stability of (2.75) is guaranteed independently of the graph and the number of the agents. However, for directed graphs, λ_i may become complex and thus the graph and the number of agents may affect stability. For example, consider a directed cyclic graph of N agents, where agent i is the only neighbor of
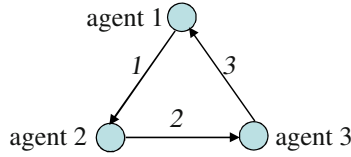
Fig. 2.4 We assign an orientation to an undirected graph of three agents, where every two agents are neighbors. The link number is put beside each link.

agent $i+1$, $i = 1, \cdots, N-1$, and agent N is the only neighbor of agent 1. For $N < 5$, (2.75) is stable. However, for $N = 5$, there exists two λ_i such that λ_i^{-1} is encircled by the Nyquist plot of $-\frac{1}{s(s+1)}$, as shown in Fig. 2.3. Thus, (2.75) becomes unstable, which implies that for directed graphs, closed-loop stability is sensitive to the graph structure and to the number of agents.   □

2.6.2 A Simulation Example

In this section, we simulate the position-based formation control system (2.74) and demonstrate that different orientations of the formation can be achieved by modifying $\mathscr{A}_k$'s.

We consider a group of three planar agents (i.e., $p = 2$), where any two agents are neighbors. As shown in Fig. 2.4, we define

$$z_1 = x_2 - x_1, \quad z_2 = x_3 - x_2, \quad z_3 = x_1 - x_3 \tag{2.80}$$

and design desired target sets for z_k's to be

$$\begin{aligned}
\mathscr{A}_1 &= \left\{ z_1 \,\middle|\, z_1 = z_1^d = [-\tfrac{\sqrt{3}}{2} \ \tfrac{1}{2}]^T \right\}, \\
\mathscr{A}_2 &= \left\{ z_2 \,\middle|\, z_2 = z_2^d = [0 \ -1]^T \right\}, \\
\mathscr{A}_3 &= \left\{ z_3 \,\middle|\, z_3 = z_3^d = [\tfrac{\sqrt{3}}{2} \ \tfrac{1}{2}]^T \right\}.
\end{aligned} \tag{2.81}$$

We choose $M = \text{diag}\{5, 2, 1\}$ and $K = 5I_3$ in (2.74). The reference velocity $v(t)$ is zero. The weight Δ in (2.73) is set to I_3. The initial positions of the agents are $x_1(0) = [5 \ 0]^T$, $x_2(0) = [2 \ 2]^T$, and $x_3(0) = [0 \ 0]^T$. Simulation result in Fig. 2.5 shows that the desired formation is achieved.
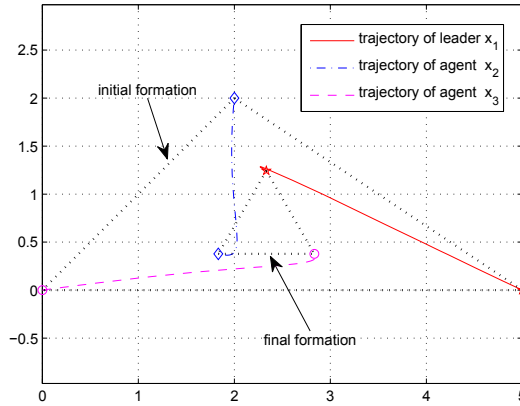
We now modify the desired target sets in (2.81) to

$$\begin{aligned}
\mathscr{A}_1 &= \left\{ z_1 \,\middle|\, z_1 = z_1^d = [-\tfrac{1}{2} \ -\tfrac{\sqrt{3}}{2}]^T \right\}, \\
\mathscr{A}_2 &= \left\{ z_2 \,\middle|\, z_2 = z_2^d = [1 \ 0]^T \right\}, \\
\mathscr{A}_3 &= \left\{ z_3 \,\middle|\, z_3 = z_3^d = [-\tfrac{1}{2} \ \tfrac{\sqrt{3}}{2}]^T \right\}.
\end{aligned} \tag{2.82}$$
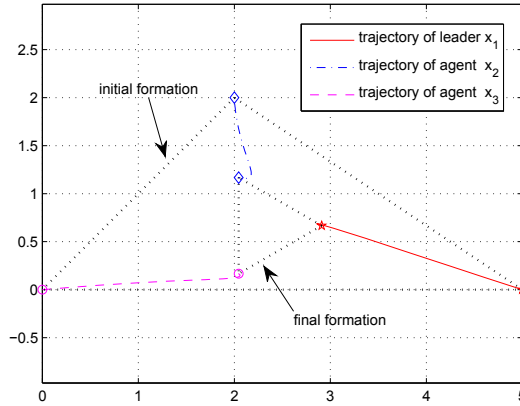
Fig. 2.5 Using (2.70) and (2.72), three agents converge to the desired formation specified in (2.81). Agents 1, 2 and 3 are denoted $\star$, $\diamond$, and $\circ$, respectively.

As shown in Fig. 2.6, (2.82) corresponds to the desired formation in Fig. 2.5 rotated counterclockwise by 90 degrees.

Fig. 2.6 Using (2.70) and (2.72), three agents converge to the desired formation specified in (2.82). Agents 1, 2 and 3 are denoted $\star$, $\diamond$, and $\circ$, respectively.

We see that the position-based formation control stabilizes both the shape and the orientation of the group formation. If the shape of the group formation is the only concern, the distance-based formation control studied in the next section is more appropriate.

2.7 Distance-based Formation Control

In this section, we study the distance-based formation control problem defined in (2.50). In contrast to the position-based formation control, this problem concerns only the shape of the group formation. It will become clear that a key complication is that Property 2.1, which holds true in the position-based formation control, is no longer satisfied in the distance-based formation control with cyclic graphs. Thus, additional undesired equilibria may arise due to the cycles in the graph, making global stabilization of the desired formation impossible. In the special case of three agents, we show that the undesired equilibria are unstable. We then conclude generic convergence to the desired formation from almost all initial conditions.

We also explore existence and uniqueness of the formation shape in this section. The existence of a formation shape is related to the requirement in (2.7), which is further sharpened to sufficient conditions on the desired target sets. These conditions are generalizations of the triangle inequality. We explore the uniqueness issue using a four-agent example. If the shape of the desired formation is a rectangle, specifying desired relative distances of the four sides is not sufficient since the agents may reach a parallelogram instead. In this case, desired relative distances of the diagonal links must also be specified to ensure that the rectangle shape is the unique desired formation.

2.7.1 Passivity-based Design

We assume that Step 1 of the passivity-based design has been achieved. We now proceed to Step 2 and design the nonlinearities ψ_k's. The control objective is to stabilize a formation where the relative distances $|z_k|$, $k = 1, \cdots, \ell$, are equal to $d_k > 0$. We choose $\mathscr{G}_k$ to be $\mathbb{R}^p \setminus \{0\}$ and let the potential functions P_k be a function of z_k satisfying (2.27)-(2.31). An example of $P_k(z_k)$ is given by

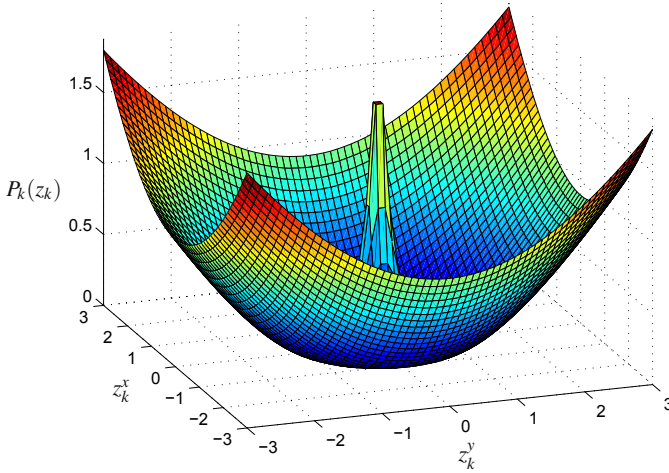$$P_k(z_k) = \int_{d_k}^{|z_k|} \sigma_k(s) ds \qquad (2.83)$$

where $\sigma_k : \mathbb{R}_{>0} \to \mathbb{R}$ is a C^1, strictly increasing function such that

$$\sigma_k(d_k) = 0, \qquad (2.84)$$

and such that, as $|z_k| \to 0$ and as $|z_k| \to \infty$, $P_k(z_k) \to \infty$ in (2.83). An illustration of $P_k(z_k)$ is shown in Fig. 2.7, where

$$\sigma_k(s) = \frac{1}{d_k} - \frac{1}{s}, \qquad (2.85)$$

$$P_k(z_k) = \frac{|z_k|}{d_k} - \ln \frac{|z_k|}{d_k} - 1 \qquad (2.86)$$

Fig. 2.7 The shape of $P_k(z_k)$: The minima of $P_k(z_k) = |z_k| - \ln|z_k| - 1$ occur on the unit circle $|z_k| = d_k = 1$. The peak at the origin guarantees the collision avoidance between the linked agents.

and d_k is set to 1. Note that the condition $P_k(z_k) \rightarrow \infty$ as $|z_k| \rightarrow 0$ is imposed only to ensure collision avoidance between linked agents. Since $P_k(z_k)$ satisfies (2.27)-(2.31), the feedback law u_i in (2.23) with the interaction forces

$$\psi_k(z_k) = \nabla P_k(z_k) = \sigma_k(|z_k|)\frac{1}{|z_k|}z_k \quad z_k \neq 0 \tag{2.87}$$

guarantees global asymptotic stability of the desired formation from Theorem 2.1 when the graph G is acyclic.

For cyclic graphs, we need to examine whether or not Property 2.1 is satisfied. We consider an example of three agents, where each agent is a neighbor of the other two agents, thereby forming a cycle in the graph G. Let the desired formation be an equilateral triangle shown in 2.8(a) with $d_k = 1$, $k = 1, 2, 3$. Note that $\psi_k(z_k)$ in (2.87) plays the role of a "spring force" which creates an attraction force when $|z_k| > 1$ and a repulsion force when $|z_k| < 1$. When $u_i = 0$, additional equilibria arise when the point masses are aligned as in Fig. 2.8(b), and the attraction force between the two distant masses counterbalances the repulsion force due to the intermediate mass.

To characterize such equilibria, we let the middle agent in Fig. 2.8(b) be agent 2 and define

$$z_1 = x_1 - x_2 \quad z_2 = x_2 - x_3 \quad \text{and} \quad z_3 = x_1 - x_3, \tag{2.88}$$

which implies from (2.6) that
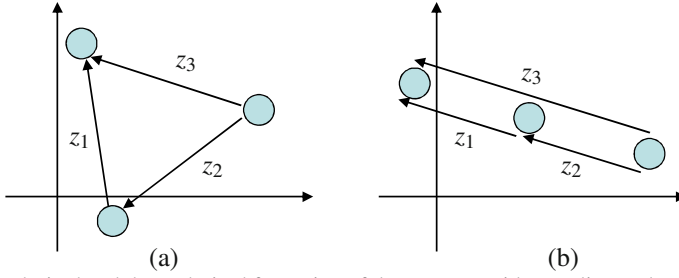
Fig. 2.8 The desired and the undesired formation of three agents with a cyclic graph: The desired formation is the equilateral triangle as (a) and the undesired formation (b) is a line.

$$D = \begin{pmatrix} 1 & 0 & 1 \\ -1 & 1 & 0 \\ 0 & -1 & -1 \end{pmatrix}. \tag{2.89}$$

The set of equilibria, given in (2.33), indicates that

$$\psi(z) = [\psi_1(z_1)^T, \psi_2(z_2)^T, \psi_3(z_3)^T]^T \in \mathcal{N}(D \otimes I_p). \tag{2.90}$$

A simple computation of the null space of D yields

$$\psi_1(z_1) = \psi_2(z_2) \tag{2.91}$$
$$\psi_1(z_1) = -\psi_3(z_3). \tag{2.92}$$

Since the undesired formation in Fig. 2.8(b) is collinear, $\frac{z_k}{|z_k|}$'s are the same. We then use (2.87) to reduce (2.91) and (2.92) to

$$\sigma_1(|z_1|) = -\sigma_3(|z_3|) \tag{2.93}$$
$$\sigma_1(|z_1|) = \sigma_2(|z_2|), \tag{2.94}$$

which have a unique solution $(|z_1| = s_1^*, |z_2| = s_2^*, |z_3| = |z_1 + z_2| = s_1^* + s_2^*)$ since $\sigma_k(\cdot)$, $k = 1, 2, 3$ are increasing and onto. Thus, the set of points where $|z_1| = s_1^*$, $|z_2| = s_2^*$ and $|z_3| = s_1^* + s_2^*$ constitute new equilibria as in Figure 2.8(b) and such desired cannot be eliminated with the choice of the function $\sigma_k(\cdot)$. Property 2.1 then fails in this formation control design and global stabilization of the desired formation is not possible for cyclic graphs.

For agents modeled as double integrators with uniform mass and damping, the following example proves that the undesired equilibria in Fig. 2.8(b) are unstable. In fact, this instability result can be extended to any graph that contains only one cycle. We refer interested readers to [9] for details.

Example 2.4 (Instability of the undesired formation of three agents).
Consider the undesired formation in Fig. 2.8(b). We first find out s_1^* and s_2^* from (2.93) and (2.94). We take $\sigma_k(\cdot)$, $k = 1, 2, 3$, as in (2.85) with $d_k = 1$. It follows from

(2.93) and (2.94) that

$$1 - \frac{1}{s_1^*} = -(1 - \frac{1}{s_1^* + s_2^*}) \tag{2.95}$$

and

$$s_1^* = s_2^*, \tag{2.96}$$

which yield $s_1^* = s_2^* = \frac{3}{4}$. This means that on the undesired formation, $|z_1| = |z_2| = \frac{3}{4}$ and $|z_3| = \frac{3}{2}$.

We assume that the agents have uniform mass $m_i = 1$ in (2.16) and uniform damping $k_i = k > 0$ in (2.17). Without loss of generality, we also let $v(t) = 0$. It then follows from (2.16), (2.17), (2.26) and (2.89) that the closed-loop system for these three agents is given by

$$\ddot{x}_1 + k\dot{x}_1 + \psi(z_1) + \psi(z_3) = 0 \tag{2.97}$$
$$\ddot{x}_2 + k\dot{x}_2 - \psi(z_1) + \psi(z_2) = 0 \tag{2.98}$$
$$\ddot{x}_3 + k\dot{x}_3 - \psi(z_2) - \psi(z_3) = 0 \tag{2.99}$$

where $\psi(z_k)$ is obtained from (2.87) and (2.85) as

$$\psi(z_k) = \frac{|z_k| - 1}{|z_k|^2} z_k. \tag{2.100}$$

To show the instability of the undesired formation, we linearize the closed-loop system around the undesired formation $\dot{x}_i = 0$, $i = 1, 2, 3$ and $z_k = z_k^u$, $k = 1, 2, 3$, where z_k^u denotes an undesired equilibrium of z_k. Letting $\delta z_k = z_k - z_k^u$, $k = 1, 2, 3$, we obtain the linearized dynamics:

$$\begin{pmatrix} \ddot{x}_1 \\ \ddot{x}_2 \\ \ddot{x}_3 \\ \dot{\delta z_1} \\ \dot{\delta z_2} \\ \dot{\delta z_3} \end{pmatrix} = \underbrace{\left(\begin{array}{ccc|ccc} -kI_p & \mathbf{0}_p & \mathbf{0}_p & -\frac{\partial \psi}{\partial z}\big|_{z_1^u} & \mathbf{0}_p & -\frac{\partial \psi}{\partial z}\big|_{z_3^u} \\ \mathbf{0}_p & -kI_p & \mathbf{0}_p & \frac{\partial \psi}{\partial z}\big|_{z_1^u} & -\frac{\partial \psi}{\partial z}\big|_{z_2^u} & \mathbf{0}_p \\ \mathbf{0}_p & \mathbf{0}_p & -kI_p & \mathbf{0}_p & \frac{\partial \psi}{\partial z}\big|_{z_2^u} & \frac{\partial \psi}{\partial z}\big|_{z_3^u} \\ \hline I_p & -I_p & \mathbf{0}_p & \mathbf{0}_p & \mathbf{0}_p & \mathbf{0}_p \\ \mathbf{0}_p & I_p & -I_p & \mathbf{0}_p & \mathbf{0}_p & \mathbf{0}_p \\ I_p & \mathbf{0}_p & -I_p & \mathbf{0}_p & \mathbf{0}_p & \mathbf{0}_p \end{array} \right)}_{\mathbf{A}} \begin{pmatrix} \dot{x}_1 \\ \dot{x}_2 \\ \dot{x}_3 \\ \delta z_1 \\ \delta z_2 \\ \delta z_3 \end{pmatrix} \tag{2.101}$$

$$= \left(\begin{array}{c|c} \mathbf{A_{11}} & \mathbf{A_{12}} \\ \hline \mathbf{A_{21}} & \mathbf{A_{22}} \end{array} \right) \begin{pmatrix} \dot{x}_1 \\ \dot{x}_2 \\ \dot{x}_3 \\ \delta z_1 \\ \delta z_2 \\ \delta z_3 \end{pmatrix} \tag{2.102}$$

where

$$\frac{\partial \psi}{\partial z}\big|_{z^u} = \frac{|z^u| - 1}{|z^u|^2} I_p + \left[-\frac{1}{|z^u|^3} + \frac{2}{|z^u|^4} \right] z^u (z^u)^T. \tag{2.103}$$

To show that the undesired formation is unstable, we only need to demonstrate that $\mathbf{A}$ has an eigenvalue with positive real part. Towards this end, we solve

$$\left(\begin{array}{c|c} \mathbf{A}_{11} & \mathbf{A}_{12} \\ \hline \mathbf{A}_{21} & \mathbf{A}_{22} \end{array}\right)\left(\begin{array}{c} \mu_1 \\ \mu_2 \end{array}\right) = \lambda\left(\begin{array}{c} \mu_1 \\ \mu_2 \end{array}\right) \tag{2.104}$$

for λ, and obtain

$$-k\mu_1 + \mathbf{A}_{12}\mu_2 = \lambda\mu_1 \tag{2.105}$$

$$\mathbf{A}_{21}\mu_1 = \lambda\mu_2. \tag{2.106}$$

Multiplying (2.105) with λ and substituting (2.106) leads to

$$\lambda^2\mu_1 + k\lambda\mu_1 - \mathbf{A}_{12}\mathbf{A}_{21}\mu_1 = 0. \tag{2.107}$$

By choosing μ_1 as the eigenvectors of $\mathbf{A}_{12}\mathbf{A}_{21}$, we obtain the eigenvalues of $\mathbf{A}$ as the solutions to the following equations

$$\lambda^2 + k\lambda - \bar{\lambda}_i = 0, \quad k > 0, \quad i = 1, \cdots, 3p \tag{2.108}$$

where $\bar{\lambda}_i$ is the ith eigenvalue of $\mathbf{A}_{12}\mathbf{A}_{21}$.

We next compute

$$\mathbf{A}_{12}\mathbf{A}_{21} = \begin{pmatrix} -\frac{\partial\psi}{\partial z}\big|_{z_1^u} - \frac{\partial\psi}{\partial z}\big|_{z_3^u} & \frac{\partial\psi}{\partial z}\big|_{z_1^u} & \frac{\partial\psi}{\partial z}\big|_{z_3^u} \\ \frac{\partial\psi}{\partial z}\big|_{z_1^u} & -\frac{\partial\psi}{\partial z}\big|_{z_1^u} - \frac{\partial\psi}{\partial z}\big|_{z_2^u} & \frac{\partial\psi}{\partial z}\big|_{z_2^u} \\ \frac{\partial\psi}{\partial z}\big|_{z_3^u} & \frac{\partial\psi}{\partial z}\big|_{z_2^u} & -\frac{\partial\psi}{\partial z}\big|_{z_3^u} - \frac{\partial\psi}{\partial z}\big|_{z_2^u} \end{pmatrix}. \tag{2.109}$$

Note from (2.103) that $\frac{\partial\psi}{\partial z}\big|_{z_k^u}$, $k = 1, 2, 3$, are symmetric. Thus, $\mathbf{A}_{12}\mathbf{A}_{21}$ is also symmetric. Then if the matrix $\mathbf{A}_{12}\mathbf{A}_{21}$ has a positive eigenvalue, there exists a positive root of (2.108) and therefore $\mathbf{A}$ is unstable.

To show that $\mathbf{A}_{12}\mathbf{A}_{21}$ has a positive eigenvalue, we recall that on the undesired formation, z_k^u's are collinear, which means that there exists a $\tilde{z} \in \mathbb{R}^p$ such that $\tilde{z} \perp z_k^u$, $\forall k$. This implies from (2.103) that

$$\frac{\partial\psi}{\partial z}\big|_{z^u}\tilde{z} = \frac{|z^u| - 1}{|z^u|^2}\tilde{z}. \tag{2.110}$$

Choosing $\zeta = [a\ b\ c]^T \otimes \tilde{z}$, where the scalars a, b, c will be specified later, and using (2.110), we obtain

$$\mathbf{A}_{12}\mathbf{A}_{21}\zeta = \left[\begin{pmatrix} -\frac{|z_1^u|-1}{|z_1^u|^2} - \frac{|z_3^u|-1}{|z_3^u|^2} & \frac{|z_1^u|-1}{|z_1^u|^2} & \frac{|z_3^u|-1}{|z_3^u|^2} \\ \frac{|z_1^u|-1}{|z_1^u|^2} & -\frac{|z_1^u|-1}{|z_1^u|^2} - \frac{|z_2^u|-1}{|z_2^u|^2} & \frac{|z_2^u|-1}{|z_2^u|^2} \\ \frac{|z_3^u|-1}{|z_3^u|^2} & \frac{|z_2^u|-1}{|z_2^u|^2} & -\frac{|z_2^u|-1}{|z_2^u|^2} - \frac{|z_3^u|-1}{|z_3^u|^2} \end{pmatrix}\begin{pmatrix} a \\ b \\ c \end{pmatrix}\right] \otimes \tilde{z}. \tag{2.111}$$
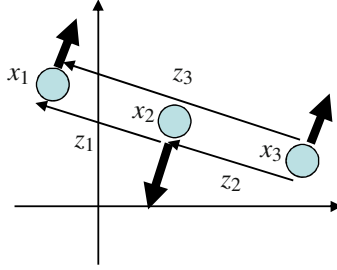
Fig. 2.9 The unstable eigenvector of the undesired formation corresponds to motion in the direction indicated by the bold arrows.

We now substitute $|z_1^u| = |z_2^u| = \frac{3}{4}$ and $|z_3^u| = \frac{3}{2}$ into (2.111) and get

$$\mathbf{A}_{12}\mathbf{A}_{21}\zeta = \left[\underbrace{\begin{pmatrix} \frac{2}{9} & -\frac{4}{9} & \frac{2}{9} \\ -\frac{4}{9} & \frac{8}{9} & -\frac{4}{9} \\ \frac{2}{9} & -\frac{4}{9} & \frac{2}{9} \end{pmatrix}}_{\mathbf{B}} \begin{pmatrix} a \\ b \\ c \end{pmatrix} \right] \otimes \tilde{z}. \tag{2.112}$$

The matrix $\mathbf{B}$ has a positive eigenvalue $\bar{\lambda} = \frac{4}{3}$ associated with an eigenvector $[-1 \ 2 \ -1]^T$. By choosing $[a \ b \ c]^T = [-1 \ 2 \ -1]^T$, we rewrite (2.112) as

$$\mathbf{A}_{12}\mathbf{A}_{21}\zeta = \bar{\lambda}\zeta, \tag{2.113}$$

which shows that $\mathbf{A}_{12}\mathbf{A}_{21}$ has a positive eigenvalue $\bar{\lambda}$. Therefore, the undesired formation in 2.8(b) is unstable.

The unstable eigenvector $[-1 \ 2 \ -1]^T \otimes \tilde{z}$ corresponds to motion in the direction shown by the bold arrows in Fig. 2.9. We interpret the unstable growth in this direction by returning to the mass-spring analogy. Since $|z_1^u| = |z_2^u| < 1$ and $|z_3^u| > 1$, springs 1 and 2 are squeezed while spring 3 is stretched. The motion in Fig. 2.9 increases $|z_1|$ and $|z_2|$ towards their natural length of one. $\square$

Because the undesired formation in Fig. 2.8(b) is unstable, we conclude generic convergence to the desired formation in Fig. 2.8(a) from all initial conditions except for those that lie on the stable manifolds of the unstable equilibria. The numerical example in Fig. 2.10 shows the convergence to the desired formation with the design (2.16) and (2.17) for three agents. In this example, the reference velocity $v(t)$ is chosen as $[0.1 \ 0.1]^T$.
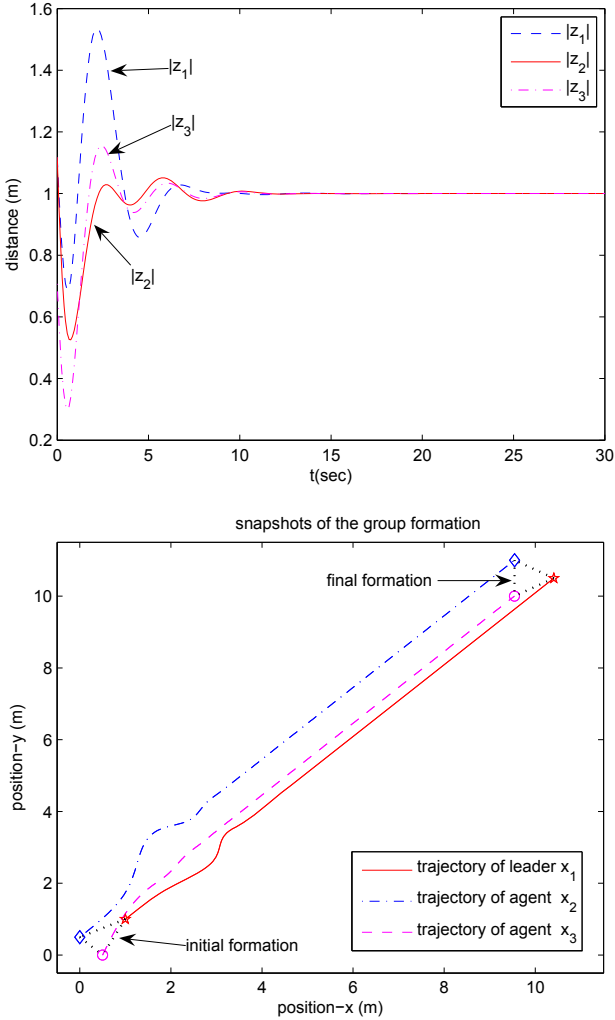
Fig. 2.10 Snapshots of the formation for the passivity-based design (2.16) and (2.17): The three relative positions, z_1, z_2 and z_3 denote $x_1 - x_2$, $x_3 - x_1$ and $x_2 - x_3$. The agents x_1, x_2 and x_3 are represented by $\star$, $\diamond$ and $\circ$, respectively.

2.7.2 Existence and Uniqueness of a Formation Shape

A key consideration in the distance-based formation control problem is whether a given set of desired relative distances d_k's, even admits an equilibrium in the closed loop, and, if so, whether the equilibrium is unique.
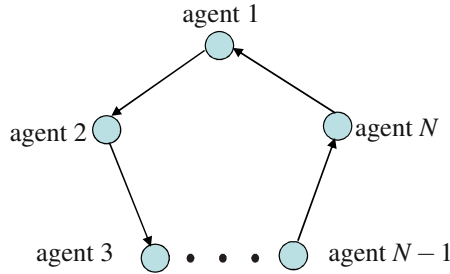
Fig. 2.11 The ring graph of N agents. The directions of the N links are assigned such that the positive end of each link is the negative end of the next link in the sequence.

Given d_k's, a desired formation equilibrium exists if the constraint (2.7) is satisfied. If the graph is acyclic, (2.7) holds for any $d_k > 0$, $k = 1, \cdots, \ell$. So we only need to consider the cyclic graph case.

As an example, consider a group of N agents that form a ring graph, i.e., each agent has exactly two neighbors. A ring graph has only one cycle and the numbers of links and nodes are the same, i.e., $N = \ell$. As shown in Fig. 2.11, we assign the orientation of the ring graph such that the positive end of each link is the negative end of the next link in the sequence. We define $z_i = x_{i+1} - x_i$, $\forall i = 1, \cdots, N-1$ and $z_N = x_1 - x_N$, and obtain

$$z_j = - \sum_{k=1, k \neq j}^{N} z_k, \quad \forall j. \tag{2.114}$$

This equality must be satisfied at the desired formation. Therefore, we obtain

$$|z_j| = \left| \sum_{k=1, k \neq j}^{N} z_k \right| \leq \sum_{k=1, k \neq j}^{N} |z_k|, \quad \forall j \tag{2.115}$$

$$\Rightarrow d_j \leq \sum_{k=1, k \neq j}^{N} d_k, \quad \forall j. \tag{2.116}$$

When $N = 3$ and the desired formation is a triangle, (2.116) reduces to the triangle inequality, that is, the sum of the lengths of any two sides of the triangle must be greater than the length of the other side. Thus, the choice of d_k is constrained by (2.116). If the graph contains multiple cycles, multiple constraints similar to (2.116) must be satisfied for d_k's so that a desired formation exists.

Once we establish that a desired formation exists for a given set of d_k's, the shape of the desired formation may not be unique if we do not specify enough number of desired relative distances. We illustrate this using a four-agent example below. More formal analysis on the uniqueness of a formation shape using "rigidity" can be found in [101, 46, 72, 43].

Example 2.5 (Stabilizing a rectangle formation of four agents).
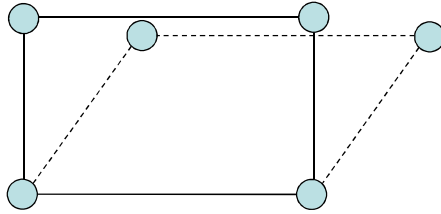
Fig. 2.12 The square formation can collapse to a parallelogram or eventually to a line.
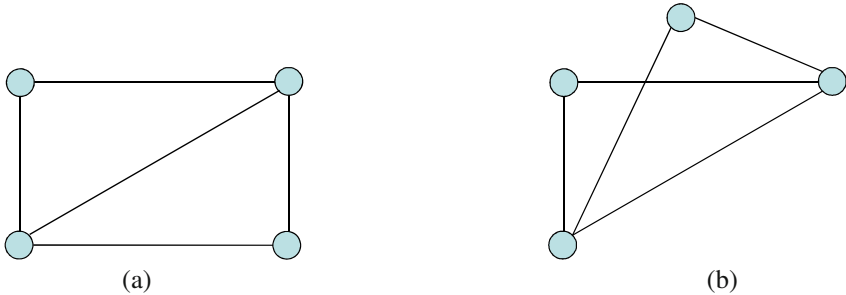
Fig. 2.13 Two possible desired formations when one diagonal link is specified.

Suppose that we want to stabilize four agents to a rectangle formation (solid lines in Fig. 2.12). Initially, we only specify the desired relative distances of the four sides. As illustrated in Fig. 2.12, the agents may converge to a rectangle or to a parallelogram or even to a line since all those shapes are in the target set (2.50). In fact, there exist infinitely many formations (up to rigid translation and rotation) in (2.50). Thus, specifying the lengths of four sides is not enough to guarantee the desired rectangle formation (up to rigid translation and rotation).

We then add a diagonal link and specify its length. Then there exist only two possible formations (up to rigid translation and rotation) in Fig. 2.13. Thus, if the agents converge to the target set (2.50), they will converge to either of the two shapes in Fig. 2.13.

If we also specify the length of the other diagonal link as shown in Fig. 2.14, we eliminate the existence of the formation in Fig. 2.13(b). In this case, if the agents converge to the desired equilibria, they converge to the desired rectangle formation.

□

2.8 Distance-based or Position-based?

We have seen two types of formation control, both of which can be designed with the passivity-based framework. We now present a comparison between these two
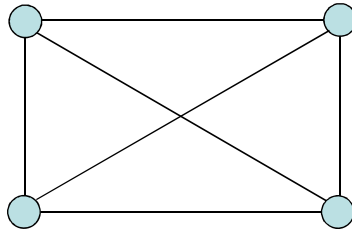
Fig. 2.14 If we specify the desired lengths of all the links, the desired formation is unique.
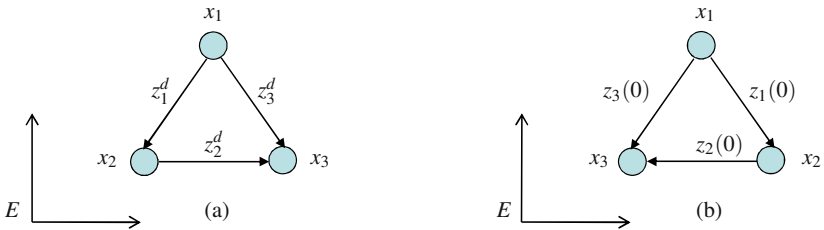
Fig. 2.15 (a) Desired formation in terms of z_k^d, $k = 1, 2, 3$. (b) Initial formation of the three agents. Even if the initial formation (b) is an equilateral triangle, agents 2 and 3 will still swap their positions to match the desired formation in (a).

formulations and illustrate the situations under which one formulation is preferable to the other.

● *Equilibria.*

For the distance-based formation control, the desired equilibria in (2.50) are spheres while for the position-based formation control, the desired equilibrium in (2.51) is a single point. The difference in these equilibria sets reflects different control objectives. When the agents need to maintain specific bearings and distances with respect to their neighbors, the position-based formation control is more suitable. In the case where cooperative tasks only require the shape of the formation rather than a specific orientation of the formation, the distance-based formation control is preferable. This is because the position-based formation control may put stringent constraints on relative positions and sacrifice the flexibility of the group motion, as we illustrate below.

Example 2.6. Consider a group of three agents $x_i \in \mathbb{R}^2$, $i = 1, 2, 3$. Suppose that the desired formation is an equilateral triangle with side length 1. One way to achieve this desired formation is to apply the position-based formation control by specifying desired relative positions between agents. We let $z_1 = x_2 - x_1$, $z_2 = x_3 - x_2$ and $z_3 = x_3 - x_1$, and choose $z_1^d = [-\frac{1}{2} \ -\frac{\sqrt{3}}{2}]$, $z_2^d = [1 \ 0]^T$ and $z_3^d = [\frac{1}{2} \ -\frac{\sqrt{3}}{2}]^T$ in the frame of E, as in Figure 2.15(a).

Let the initial formation of the three agents shown in Figure 2.15(b) be $z_1(0) = z_3^d$, $z_2(0) = -z_2^d$ and $z_3(0) = z_1^d$, which means that it is already an equilateral triangle with side length 1. However, this equilateral formation does not match the desired targets (2.51). Since (2.51) is globally attractive by the position-based formation
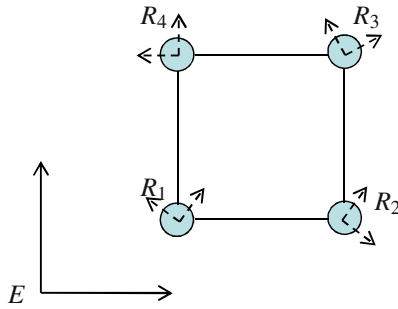
Fig. 2.16 Four planar agents in a global frame E: R_i represents a local frame for agent i. The desired formation is shown as an equilateral square.

control design, the agents will start moving away from the initial formation in Figure 2.15(b) towards the desired formation in Figure 2.15(a), which results in unnecessary time and control energy consumption.   □

- *Control Design and Stability.*

    The difference in equilibria leads to different control designs: The design in Section 2.7.1 employs nonlinear potential functions to achieve the distance-based formation control while position-based formation control can be realized by linear feedback laws, such as the design in (2.74).

    Moreover, because of the difference in equilibria sets, the distance-based formation control stabilizes the desired formation only locally when the graph contains cycles while the position-based formation control is able to globally stabilize the desired formation. This is because Property 2.1 is satisfied for the position-based formation control but not for the distance-based formation control. Because the position-based formation control is globally stabilizable, it has been applied to different cooperative control problems, including formation control of unicycles [83, 41].

- *Desired Formation Specification.*

    The difference in the equilibria sets (2.50) and (2.51) also results in different specifications of the desired formation. For example, consider four planar agents in Fig. 2.16. The coordinate E is a global frame while R_i, $i = 1, \cdots, 4$, is agent i's local frame, possibly different from E. The desired formation is an equilateral square shown in Fig. 2.16. To specify a desired formation using (2.50), one only needs to determine the desired relative distances, which is invariant in different frames. This implies that the desired distances can be specified in either E or R_i's. However, for position-based formation control, the desired relative position z^d must be prescribed in one common frame, such as E in Fig. 2.16.

    One subtlety in specifying a desired formation is how to guarantee a *unique* desired formation. For position-based formation control, specifying desired relative positions of $N-1$ links is sufficient if these $N-1$ links can form a connected graph. This is because once the desired relative positions of these $N-1$ links are fixed, the desired relative positions between any two agents are also fixed. As an illustration,

consider Fig. 2.16 and suppose that we specify the relative positions for the links between agents 1 and 2, between agents 2 and 3, and between agents 3 and 4. These three links form a connected graph and thus all the other relative positions, such as relative positions between agents 4 and 1, between agents 2 and 4, are uniquely determined. However, for distance-based formation control, specifying the desired lengths of $N-1$ links may not enough to ensure a unique formation, as we already illustrated in Example 2.5.

• *Implementation of Control Laws.*

In practice, the relative position z_k's are obtained in each agent's local frame. If precise global frame information is available, the agents may transform the local measurements of z_k to the global coordinates for implementation. However, in some applications, such as space interferometry sensing, the global frame information may be imprecise or unavailable. In this case, we show that distance-based formation control can be easily implemented without knowledge of any global frame information while position-based formation control requires the knowledge of a common frame in which the desired relative positions z^d are specified.

For illustration, we assume double integrator dynamics for the agents and rewrite the control laws for distance-based and position-based formation control as

$$\text{position-based:} \quad \ddot{x}_i = \tau_i = -k_i \dot{x}_i - \sum_{i=1}^{\ell} d_{ik}(z_k - z_k^d) \tag{2.117}$$

$$\text{distance-based:} \quad \ddot{x}_i = \tau_i = -k_i \dot{x}_i - \sum_{i=1}^{\ell} d_{ik} \log\left(\frac{|z_k|}{d_k}\right)\frac{1}{|z_k|}z_k \tag{2.118}$$

where we take $v(t) = 0_p$. Suppose that (2.117)-(2.118) are written in a global frame E. Then z_k^d's must be specified in E. When E is not available, each agent implements ${}^i\tau_i$, the τ_i vector represented in agent i's frame[2]. Let R_i be the agent i's frame represented in E. Then ${}^i\tau_i$'s are given by

$$\text{position-based:} \quad {}^i\tau_i = -k_i R_i^T \dot{x}_i - \sum_{i=1}^{\ell} d_{ik}(R_i^T z_k - R_i^T z_k^d) \tag{2.119}$$

$$\text{distance-based:} \quad {}^i\tau_i = -k_i R_i^T \dot{x}_i - \sum_{i=1}^{\ell} d_{ik} \log\left(\frac{|z_k|}{d_k}\right)\frac{1}{|z_k|}R_i^T z_k. \tag{2.120}$$

It then becomes evident that both (2.119) and (2.120) require agent i's velocity represented in R_i (i.e., the term $R_i^T \dot{x}_i$) and the relative position z_k represented in R_i (i.e., the term $R_i^T z_k$). In addition, the position-based formation control also needs $R_i^T z_k^d$, which cannot be computed if the global frame E is not known. Thus, we conclude that distance-based formation control is more suitable for applications with no global frame information.

---

[2] For vector representations in different frames, we refer readers to Appendix B.12.1.

2.9 Summary

In this chapter, we employed passivity as a design tool for a class of group co-ordination problems where the topology of information exchange between agents is bidirectional. We exploited the symmetry inherent in the undirected graph and represented it as a passivity-preserving structure (pre-multiplication of $D^T \otimes I_p$ and post-multiplication by its transpose as in Fig. 2.2). We used this structure to develop a passivity-based design framework that yields a broad class of decentralized and scalable cooperative control laws for complex and heterogeneous agent dynamics. In addition to stabilizing feedback rules, the passivity-based design framework constructs a Lur'e-type Lyapunov function. As we will illustrate in Chapters 3, 4 and 6, this Lyapunov function serves as a starting point for several adaptive designs that enhance robustness of group motion.

We next applied the passivity-based design framework to agreement problems. We developed a class of decentralized protocols that achieve agreement of agents. We also studied the position-based and the distance-based formation control. For the position-based formation control, we showed that it can be transformed to an agreement problem, which means that the desired formation is guaranteed. In the distance-based formation control, we showed that the desired formation is only locally asymptotically stable for cyclic graphs because Property 2.1 fails. We then proved the instability of the undesired formations for a three-agent example and concluded generic convergence to the desired formation. We also discussed how to specify a unique and feasible formation shape. Finally, a comparison between the position-based and the distance-based formation control was presented.

2.10 Notes and Related Literature

• The use of Schur decomposition in Example 2.3 follows [47, Theorem 3].

• The passivity-based framework in this chapter was developed in [5].

• Related Literature on agreement and formation control: A rapidly-growing literature has been witnessed in the field of agreement. See e.g., [102, 109] for a summary. Applications of formation control can be found in the survey papers [117, 118, 26, 93]. Reference [98] first applied potential function method to the formation control with undirected information topology. A flocking algorithm was studied in [131] under time-varying communication graphs. In [47], the formation of multiple vehicles with linear identical dynamics was investigated. Based on a decentralized simultaneous estimation and control framework, the authors in [150] studied formation control using geometric moments. In [44], the position-based formation control was formulated as an optimization problem and a distributed receding horizon controller was proposed. Reference [123] considered optimal formation control of linear agent dynamics by using relative position and communicating estimates. In [124], a parallel estimator was developed for controlling formation of linear dynamical agents with directed graphs. Reference [152] employed Jacobi shape theory

to decouple translational formation dynamics from shape and orientation dynamics. The proposed cooperative control laws locally stabilize the desired formation shape. Formation control with directed graphs has also been investigated in [22, 23, 55, 4].

• For directed graphs, significant results have been obtained using a number of different approaches, such as the use of Laplacian properties for directed graphs in [103, 47, 109, 79], input-to-state stability [135], passive decomposition of group dynamics [76], eigenvalue structure of circulant matrices [87], set-valued Lyapunov theory in [90], and contraction analysis [31, 32]. In particular, recent research in [29, 28] also employed passivity as a tool for agreement of nonlinear systems. The results [29, 28] are applicable to strongly connected directed graphs for relative degree one agents. The passivity-based framework in this book allows agent dynamics to be relative degree higher than one for undirected graphs.

• Step 1 in the passivity-based framework may not be applicable to certain classes of dynamical systems, such as nonholonomic agents. Significant research has been conducted when the agents are modeled as unicycles. In [77], the authors considered a group of unit speed unicycles and proposed designs to achieve different group formations. A leader-following approach was introduced in [48] to ensure a desired group formation, where each unicycle maintains desired relative bearings and distances with respect to its neighbors. The control algorithms were based input-output linearization. Reference [88] studied cooperative formation control of multiple unicycles by assigning each agent a desired trajectory to track. The tracking errors decrease as feedback gains increase. In [83], formation control of unicycles was studied in the position-based formulation and necessary and sufficient graphical conditions were obtained. Reference [87] employed eigenvalue structure of circulant matrices in cyclic pursuit formation. Agreement of positions and orientations of unicycles was considered in [37] and discontinuous time-invariant control laws were analyzed using nonsmooth analysis. For dynamical nonholonomic agents, backstepping is a useful tool to transform coordination laws from kinematic level to dynamic level [42, 39]. In [50], formation control with general agent dynamics was formulated as a nonlinear output regulation problem.